Ku80 autoantigen as a cellular coreceptor for human parvovirus B19 infection

Yasuhiko Munakata, Takako Saito-Ito, Keiko Kumura-Ishii, Jie Huang, Takao Kodera, Tomonori Ishii, Yasuhiko Hirabayashi, Yoshio Koyanagi, and Takeshi Sasaki

Human parvovirus B19 (B19) infects human erythroid cells expressing P antigen. However, some cell lines that were positive for P antigen failed to bind B19, whereas some cell lines had an ability to bind B19 despite undetectable expression of P antigen. We here demonstrate that B19 specifically binds with Ku80 autoantigen on the cell surface. Furthermore, transfection of HeLa cells with the gene of Ku80 enabled the binding of B19 and allowed its entry into cells. Moreover, reduction of cell-surface expression of Ku80 in KU812Ep6 cells, which was a high-sensitive cell line for B19 infection, by short interfering RNA for Ku80 resulted in the marked inhibition of B19 binding in KU812Ep6 cells. Although Ku80 originally has been described as a nuclear protein, human bone marrow erythroid cells with glycophorin A or CD36, B cells with CD20, or T cells with CD3 were all positive for cell-surface expression of Ku80. B19 infection of KU812Ep6 cells and bone marrow cells was inhibited in the presence of anti-Ku80 antibody. Our data suggest that Ku80 functions as a novel coreceptor for B19 infection, and this finding may provide an explanation for the pathologic immunity associated with B19 infection. (Blood. 2005;106: 3449-3456)

Introduction

Human parvovirus B19 (B19) infects erythroid-lineage cells through P antigen and causes various clinical symptoms such as erythema infectiosum, anemia, polyarthritis, or fetal hydrops in humans.[1,2] The cellular receptor for B19 infection has been regarded as blood group P antigen based on the failure of B19 infection in a patient with an hereditary defect of P antigen.[3] However, the target cells of B19 may be not be exclusively P-antigen–positive erythroid-lineage cells, as illustrated by the poor relationship between P antigen expression levels and the efficiency of B19 infection[4] or the failure of B19 binding to globoside.[5] Recently, Weigel-Kelley et al described the role of $\alpha5\beta1$ integrin as the cellular coreceptor for B19 infection.[6] The notion that B19 receptor is not solely P antigen may be compatible with clinical findings that B19 has been detected in mononuclear cells of blood or tonsils with acute or prolonged B19 infection.[7,8] Also, following B19 infection, the numbers of peripheral blood lymphocytes may decrease despite undetectable levels of P antigen on their cell surface.[9,10] Finally, autoimmune-like phenomena including antinuclear antibodies, rheumatoid factors, or antiphospholipid antibodies are often associated with B19 infection,[8,11] and the levels of tumor necrosis factor α (TNF-α) and interferon γ (IFN-γ) secreted from macrophages or T cells are elevated during acute or prolonged B19 infection.[12] Clinical studies have shown that B19 DNA can be amplified from joint samples by polymerase chain reaction (PCR).[13,14] and infective B19 was detected in the articular lesions of patients with rheumatoid arthritis. B19 transcripts and B19 protein viral protein 1 (VP1) were also present in T cells, B cells, macrophages, and follicular dendritic cells.[14] The cellular mechanism that may allow B19 binding and its entry into nonerythroid cells has not been elucidated. In the present study, we explored a putative receptor for B19 that was distinct from P antigen.

Materials and methods

Cells

Macrophage cell lines U937, urinary bladder carcinoma cell line T24, colon cancer cell line SW620, renal adenocarcinoma cell line ACHN, and HeLa cells were provided by the Cell Resource Center for Biomedical Research, Institute of Development, Aging and Cancer, Tohoku University (Sendai, Japan). Human erythroid cell line KU812Ep6[15] was provided by E. Miyagawa (Institute of Fuji Rebio, Tokyo, Japan). T-cell line H9 was purchased from American Type Culture Collection (Manassas, VA). Bone marrow samples were obtained from the volunteers who gave informed consent for the use of their samples for our study. Informed consent was provided in accordance with the Declaration of Helsinki.

Human parvovirus B19

Serum from patient 1 with acute B19 infection was used as the source for B19 in the in vitro infection study. The serum contained 2.5×10^{14} copies of B19-DNA per milliliter but was negative for IgM and IgG anti-B19 antibodies.[16] B19 was purified using cellulose hollow fiber, was provided by Dr. K. Yamaguchi,[17] and used as an antigen for enzyme-linked immunosorbent assay (ELISA).

From the Department of Rheumatology and Hematology, and Department of Virology, Tohoku University Graduate School of Medicine, Sendai, Japan.

Submitted February 8, 2005; accepted July 5, 2005. Prepublished online as *Blood* First Edition Paper, August 2, 2005; DOI 10.1182/blood-2005-02-0536.

Supported by a Grant-in-Aid for Scientific Research (A) from the Ministry of Education, Science, Sports and Culture in Japan.

Y.M. and T.S.-I. designed with research, performed research, and wrote the paper; K.K.-I., J.H., T.K., and T.I. performed research; Y.H. analyzed data; and Y.K. and T.S. designed research.

Y.M. and T.S.-I. contributed equally to this work.

Reprints: Yasuhiko Munakata, Department of Rheumatology and Hematology, Tohoku University Graduate School of Medicine, 1-1 Seiryo-cho, Aoba-ku, Sendai 980-8574, Japan; e-mail: mnkt@mail.tains.tohoku.ac.jp.

The publication costs of this article were defrayed in part by page charge payment. Therefore, and solely to indicate this fact, this article is hereby marked "advertisement" in accordance with 18 U.S.C. section 1734.

Recombinant human parvovirus B19 empty capsid protein

Recombinant human parvovirus B19 empty capsid protein (rB19ECP), prepared as described previously,[18] was kindly provided by K. Kamata at Denka Seiken (Tokyo, Japan). rB19ECP was composed of VP1 and VP2 at a ratio of 5:95, respectively.

Antibodies

Monoclonal anti-Ku80 antibodies that recognized N-terminus (amino acids 3-22) or C-terminus of Ku80 (amino acids 610-705) were purchased from Oncogene (Boston, MA) and BD Biosciences (San Jose, CA), respectively. PAR3 is a mouse monoclonal antibody recognizing VP2, which shared with VP1 of B19.[19,20] 1F5 is a mouse monoclonal antibody with anti-idiotypic activity to an anti-DNA antibody,[21] which was used as a control for flow cytometry analysis. GL4, a rabbit polyclonal antigloboside antibody (IgG and IgM), was purchased from Matreya (State College, PA). Monoclonal anti–α5 and anti–β1 integrin antibodies were purchased from Chemicon (Temecula. CA). Other monoclonal antibodies were purchased from BD Biosciences.

In vitro infection of B19

Cells (2×10^6) in 0.5 mL RPMI were infected with B19 containing serum from 1 (diluted at 2×10^{11} copies of B19 DNA/mL) for 30 minutes on ice and washed extensively 3 times with phosphate-buffered saline (PBS), pH 7.2, for evaluation of B19 adsorption. To study B19 replication, the prepared cells in 3 mL RPMI containing 10% fetal bovine serum (FBS) were further incubated at 37°C for 48 hours in a 5% CO_2 humidified atmosphere, followed by 3 extensive washes with PBS and then evaluated for B19 protein and B19 DNA.

Protein precipitation and purification of precipitated protein

Cell-surface protein of H9 cells was labeled with sulfo-NHS esters of biotin (Pierce, Rockford, IL), followed by protein precipitation. H9 cells were treated with Nonidet P-40 lysis buffer (1% Nonidet P-40, 140 mM NaCl, 1 mM phenylmethylsulfonyl fluoride [PMSF], 5 mM EDTA [ethylenediaminetetraacetic acid], 50 mM Tris [tris(hydroxymethyl)aminomethane)–HCl, pH 7.4) and immunoprecipitated with rB19ECP- or bovine serum albumin (BSA)–conjugated cyanogen bromide (CNBr)–Sepharose (Amersham Bioscience, Piscataway, NJ). The precipitated samples were separated under denaturing conditions in a 7.5% sodium dodecyl sulfate–polyacrylamide gel electrophoresis (SDS-PAGE) gel, followed by electrotransfer to a polyvinylidene difluoride (PVDF) membrane. Protein was detected with enhanced chemiluminescence (ECL) Western blotting detection system (Amersham Biosciences) and visualized by LAS-1000 (Fujifilm, Tokyo, Japan). A crude membrane fraction of H9 cells (1×10^{11}) was prepared and solubilized in 1% Nonidet P-40 lysis buffer. The fraction was then precipitated with rB19ECP-conjugated CNBr-Sepharose for 16 hours at 4°C, and the precipitated proteins were separated by SDS-PAGE followed by Coomassie blue staining. Protein sequencing was carried out by Toray Research Center (Kamakura, Japan).

Flow cytometry analysis

Cells were suspended in 100 μL 1% BSA-PBS and incubated with 5 μg/mL test antibodies on ice for 30 minutes. Cells were then washed 3 times with PBS. Cells that required secondary antibodies for detection were further incubated with fluorescein isothiocyanate (FITC)–conjugated goat anti–mouse IgG (or FITC-conjugated anti–rabbit IgG for the GL4 primary antibody; Sigma, St Louis, MO) at 1:200 on ice for 30 minutes. Cells were washed 3 times with PBS before flow cytometry analysis (Becton Dickinson, San Jose, CA). For the detection of Ku80 on the cell surface of bone marrow cells, cells were first reacted with 5 μg/mL anti-Ku80 antibody followed by an incubation with FITC-conjugated anti–mouse IgG antibody. After being washed, cells were reacted with the cell-lineage–specific antibodies (anti–glycophorin A, anti-CD3, anti-CD20, anti-CD56, anti-CD14, or anti-CD36 antibodies) conjugated with phycoerythrin (PE; BD Biosciences) according to the manufacturer's instruction.

In the in vitro infection study, B19-infected cells were fixed with 4% paraformaldehyde followed by permeabilization with SAP buffer (0.1% saponin, 0.05% NaN_3 in Hanks balanced salt solution). Next, cells were incubated with PAR3 at a concentration of 5 mg/mL on ice for 30 minutes, followed by the same procedure as described.

ELISA and quantitative PCR

ELISA was carried out by using rB19ECP-fixed microwells (Denka Seiken). The basic protocol for ELISA and quantitative PCR for measuring B19-DNA was performed as described before.[15,16]

Preparation of cell fraction from B19-infected cells

Cells (6×10^5) were infected with B19 for 30 minutes on ice. Following three washes with PBS, pH 7.2, DNA was extracted from 2×10^5 cells to measure adsorbed B19. The remaining 4×10^5 cells were further incubated for 30 minutes at 37°C, followed by 3 washes with PBS, pH 4.5. To obtain cytoplasm fractions of B19-infected cells, cells were treated with lysis buffer A (100 mM Tris-HCl, pH 7.5, 1% Triton X-100, 5 mM EDTA, 50 mM NaCl, and 100 μM PMSF), and centrifuged. Then, DNA was extracted from the supernatant to measure B19-DNA in cytoplasm. The pellets were washed with lysis buffer A 3 times and treated with lysis buffer B (100 mM Tris-HCl, pH 7.5, 1% Triton X-100, 5 mM EDTA, 500 mM NaCl, and 100 μM PMSF). Following centrifugation, DNA was extracted from the supernatant to measure B19-DNA in nuclei.

Transfection

Five micrograms of expression vector pcD[22] containing pKu80 was used for the transfection of 1×10^5 HeLa cells, and pcD was used as a vector-only control. Transfection was done using the lipofectin method (Invitrogen, Carlsbad, CA). Transfected HeLa cells were infected with B19 for 30 minutes at 37°C. After being washed 3 times with PBS, pH 7.2, cells were collected with 5 mM EDTA-PBS, and B19 was detected by confocal microscopy analysis. Transfected HeLa cells were incubated with 1 μg/mL biotinylated rB19ECP in the presence of 5 μg/mL inhibitor antibodies for 30 minutes at 37°C. After being washed 3 times with PBS, pH 7.2, cells were collected with 5 mM EDTA-PBS, and rB19ECP or Ku80 was detected by confocal microscopy analysis.

RNA interference of K80 in KU812Ep6

The short interfering RNA (siRNA) for Ku80 was synthesized targeting the sequence between nucleotide numbers 130 and 148: 5′-CAAGCAAA-GAAGGUGAUAAdTdT-3′ (sense), 3′-dTdTGUUCGUUUCUUCCAC-UAUU-5′ (antisense). Disordered siRNA of scrambled nucleotide sequence, used as negative control, was 5′-GCGCGCUUUGUAGGAUUCG-dTdT-3′ (sense), 3′-dTdTCGCGCGAAACAUCCUAAGC-5′ (antisense). Synthesized siRNA (200 nM) was transfected to 1×10^6 KU812Ep6 cells by Cell Line Nucleofector Kit V (Amaxa, Gaithersburg, MD) according to the manufacturer's instructions. Transfected cells were subjected to flow cytometry analysis and in vitro infection study of B19, after 48 hours of incubation.

Detection of B19 in HeLa cells by confocal laser microscopy

Cells were grown on glass microslides and fixed with 4% paraformaldehyde in PBS for 10 minutes at room temperature. Cells were blocked with PBS containing 10% FBS for 30 minutes at 4°C, followed by incubation with mouse monoclonal anti-B19 antibody PAR3 (10 μg/mL) for 30 minutes at 4°C, then washed with PBS twice, and incubated with FITC-conjugated goat anti–mouse IgG (1:100; Sigma) for 30 minutes at 4°C. To detect localization of Ku80 and rB19ECP, cells on glass microslides were incubated with mouse monoclonal anti-Ku80 antibody (5 μg/mL) for 30 minutes at 4°C, washed with PBS twice, and incubated with tetramethyl isothiocyanate (TRITC)–conjugated goat anti–mouse IgG (1:50; Sigma) for 30 minutes at 4°C; cells were further incubated with avidin-FITC (1:100; Gibco, Carlsbad, CA) for 30 minutes at 4°C for the detection of labeled

rB19ECP. Confocal miscroscopy analysis was performed with a D-ECLIPSE CI (Nikon, Kawasaki, Japan) mounted with 20×/0.50 or 40×/0.75 Plan Fluor dry objective lenses. Excitation at 488 nm from an argon laser and at 543 nm from a helium-neon laser was used. Images were acquired with E2-Cl 2.00 software (Nikon) and processed with Adobe Photoshop 7.0.1 (Adobe Systems, San Jose, CA).

Results

Identification of B19-binding protein on the cell surface of nonerythroid cells

To identify a putative receptor for B19, we first checked the expression of P antigen (Figure 1). Flow cytometry analysis revealed that α5β1 integrin[6] was also positive on the surface of all cell lines tested (data not shown). We then studied the binding and replication of B19 in association with the expression of P antigen and α5β1 integrin. Quantitative study for cell-surface binding, B19 DNA replication, and fluorescence-activating cell sorting (FACS) analysis using anti–B19 protein (VP2) antibody PAR3 revealed that B19 binds not only to a P antigen–expressing erythroid cell line KU812Ep6 but also to a macrophage cell line, U937, to a T-cell line, H9, and a renal carcinoma cell line, ACHN, in which P antigen was undetectable on the cell surface. None of the cell lines, T24, SW620, and HeLa, bound B19 despite surface P antigen expression (left column in Figure 1A). FACS analysis at 48 hours after B19 infection revealed 2 types of staining patterns for B19 protein following immunohistochemistry using PAR3: (1) intense staining in KU812Ep6 and (2) weak staining in Ku812Ep6, U937, H9, and ACHN (left column in Figure 1B). Replication of B19 DNA and the synthesis of B19 protein was observed in KU812Ep6, but not in any of the other cells, irrespective of the presence of P antigen (right column in Figure 1A and right column in Figure 1B) or α5β1 integrin.

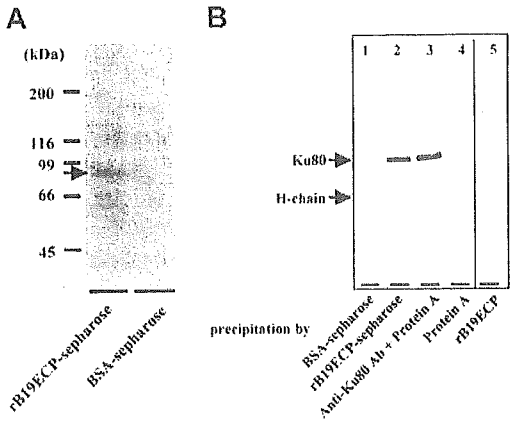

Figure 2. Determination of B19-binding protein on surface of T cell line H9. (A) Isolation of B19-binding protein from H9 surface. Surface proteins H9 of cells were biotinylated. Cell lysate from 1×10^{11} biotinylated H9 cells was mixed with rB19ECP-conjugated Sepharose or with BSA-conjugated Sepharose. Precipitated protein was isolated and reacted with streptavidin–horseradish-peroxidase conjugate on PVDF membranes, followed by the chemiluminescence detection. (B) Western blotting of protein from H9 surface with anti-Ku80 antibody. Lanes 1-4 show cell lysate precipitated with indicated protein or protein-conjugated Sepharose. Lane 5 shows the rB19ECP (1 μg) resolved by electrophoresis under denaturing conditions.

To determine the cell-surface molecule responsible for B19 binding to H9 cells, a recombinant empty capsid protein of B19 (rB19ECP) was used. Biotinylated rB19ECP bound H9 in a dose-dependent manner (data not shown). We then purified the rB19ECP-binding molecule from the cell surface of H9 using rB19ECP-conjugated Sepharose (rB19ECP-Sepharose). The precipitated 80-kDa protein (Figure 2A) was analyzed by matrix-assisted laser desorption ionization-time of flight mass spectrometry. The obtained data were collated and submitted for homology search using the Swiss Prot and NCB Inr databases. The Ku80 autoantigen was identified as the gene product with the highest

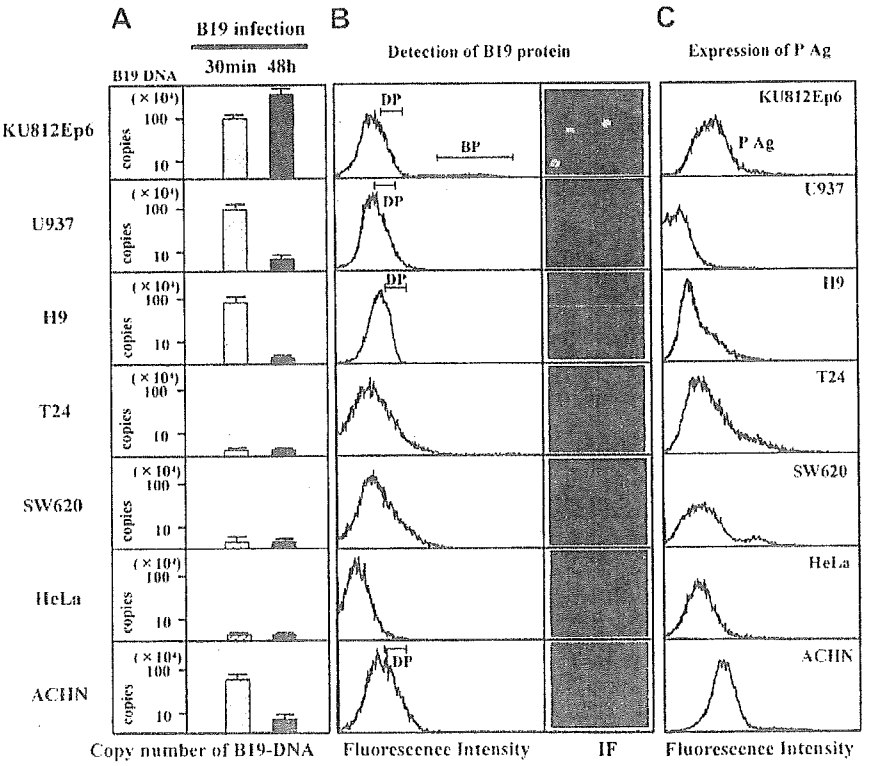

Figure 1. B19 infectivity and expression of P antigen. Each cell line (2×10^6) was inoculated with B19 (1×10^{11} copies of B19 DNA) for 30 minutes at 4°C and washed with PBS, pH 7.2, 3 times. Half of the cells in each group were used for evaluation of B19 adsorption (left column in panel A), and remaining cells in 3 mL RPMI containing 10% FBS were further incubated at 37°C for 48 hours to measure B19 DNA replication (right column in panel A) or to detect B19 protein (B). (A) B19 binding and replication of B19 in various cell lines. B19-infected cells were quantified for B19 DNA as described in "Materials and methods." The left column (▨) is regarded as B19 adsorption, and the right column (■) as B19 replication. The scale for B19 DNA is shown in logarithm. (B) Detection of B19 protein in B19-infected cells. After a 48-hour incubation with B19, the cells were washed 3 times with PBS and they were fixed with 4% paraformaldehyde followed by permeabilization with SAP buffer (0.1% saponin, 0.05% NaN_3 in Hanks balanced salt solution). Then, cells were incubated with PAR3 at a concentration of 5 μg/mL on ice for 30 minutes, followed by an incubation with FITC-conjugated goat anti–mouse IgG. The expression of B19 protein in cytoplasm was analyzed by flow cytometry with PAR3 (line) or isotype-matched antibody 1F5 (shadow; left panel), or by immunofluorescence (IF) staining with PAR3 (right panel). Two types of positive patterns were observed in flow cytometry: dull positive (DP) pattern in KU812Ep6, U937, H9, and ACHN; bright positive (BP) pattern in KU812Ep6. (C) Flow cytometry analysis of P antigen expression on the cell surface. Indicated cells were incubated with antiglobloside antibody, GL4, followed by PE-labeled anti–rabbit IgG. Shadow represents staining using rabbit IgG as a negative control.

homology in both databases. As a confirmation, the rB19ECP-binding 80-kDa protein reacted with anti-Ku80 antibody (Figure 2B). Competitive ELISA further confirmed the specific binding between Ku80 and B19. Biotinylated recombinant Ku80 (rKu80) reacted with rB19ECP fixed to microwells (Figure 3A); the binding was selectively inhibited by unlabeled rKu80 but not by recombinant Ku70 (rKu70), globoside, or recombinant soluble CD26 (sCD26)[23] (Figure 3B). This binding was also inhibited in the presence of native B19 particles from infected patients (Figure 3C). Two anti-Ku80 antibodies significantly inhibited the binding of biotinylated rKu80 and rB19ECP, whereas anti-Ku70 antibody or anti-CD106 antibody failed to inhibit the binding (Figure 3D).

Ku80 participates in B19 binding and subsequent entry

We next investigated whether Ku80 would participate in B19 binding on the cell surface and facilitate B19 entry. KU812Ep6, U937, H9, and ACHN cells efficiently bound B19 (Figure 1A) and all of these cells clearly expressed Ku80 on their surface (Figure 4A). On the other hand, Ku80 was undetectable on T24, SW620, and HeLa cells, and no binding of B19 occurred (Figures 4A and 1A). An in vitro infection experiment demonstrated efficient replication of B19 DNA in KU812Ep6 cells that expressed both Ku80 and P antigen. B19 failed to amplify itself in U937, H9, and ACHN cells, which express Ku80 but no detectable levels of P antigen on the cell surface (Figures 1 and 4A). T24, SW620, and HeLa cells were nonpermissive for B19 infection although they expressed P antigen (Figure 1) and α5β1 integrin.

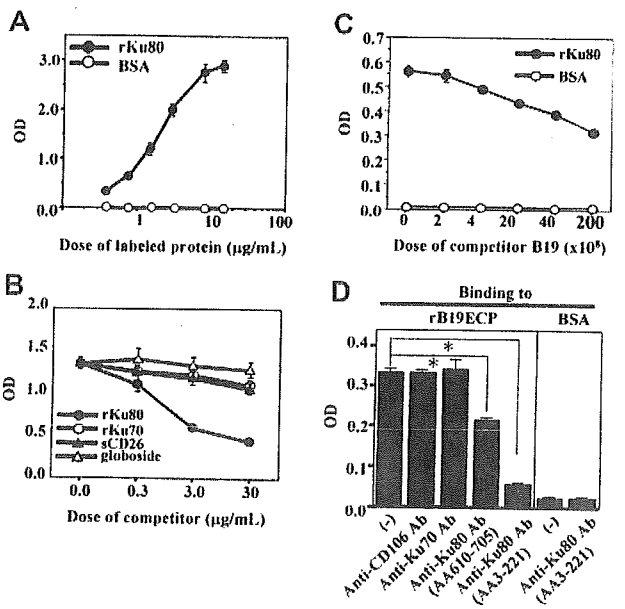

Figure 3. Specific binding of rB19ECP to Ku80. (A) Specific binding of Ku80 to rB19ECP. Indicated concentration of biotinylated rKu80 or biotinylated BSA was reacted with rB19ECP fixed to 96 microwells and detected by ELISA. (B) Competitive ELISA for rB19ECP binding to rKu80. Biotinylated rKu80 (2 μg/mL) was reacted with rB19ECP fixed to wells in the presence of indicated doses of unlabeled rKu80, rKu70, sCD26, or globoside. (C) Inhibition of rB19ECP binding to rKu80 by purified B19. Biotinylated rKu80 (1 μg/mL) was added to rB19ECP fixed to wells in the presence of B19 that was purified from B19+ serum with repeated microfiltration. Doses of B19 are expressed as copy numbers of B19 DNA. (D) Inhibition of rB19ECP binding to rKu80 by anti-Ku80 antibodies. Binding of biotinylated rKu80 or biotinylated BSA to rB19ECP fixed to wells was measured in the presence of isotype-matched mouse monoclonal antibodies as indicated.

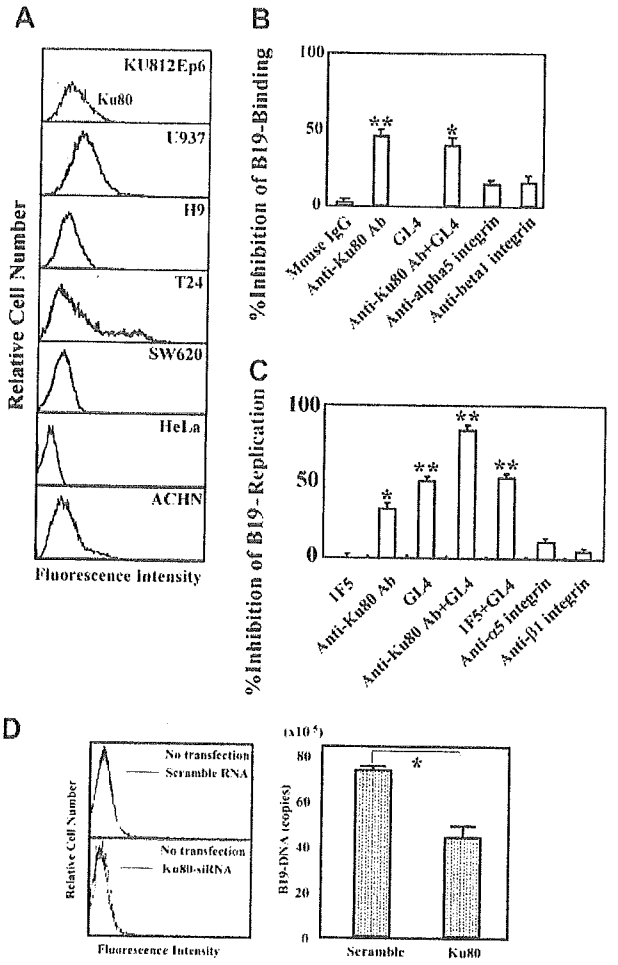

Figure 4. Role of Ku80 in B19 infection in vitro. (A) Ku80 expression on cell surface. The indicated cell lines were reacted with 5 μg/mL mouse monoclonal anti-Ku80 antibody (line) or 5 μg/mL isotype-matched mouse monoclonal antibody 1F5 (shadow), followed by FITC-labeled anti–mouse IgG antibodies. Cells were washed with PBS, and cell-surface expression of Ku80 was analyzed by flow cytometry. (B) Blocking of B19 adsorption by anti-Ku80 antibody or antigloboside antibody. KU812Ep6 cells (2×10^6) were infected with B19 (2×10^{11} copies of B19 DNA) on ice for 30 minutes in the presence of the indicated antibodies (5 μg/mL) and extensively washed with PBS 3 times. To activate α5β1 integrin, anti-integrin antibodies were used in the presence of divalent ions (1 mM Mn^{2+}, 1 mM Mg^{2+}). B19 DNA in each group was quantified by quantitative PCR. The blocking ability of B19 binding by each antibody was expressed as percent decrease of B19-DNA in each group compared to that in antibody-untreated cells. $^{**}P < .01$, $^{*}P < .05$ by Student *t* test. (C) Blocking of B19 replication by anti-Ku80 antibody or antigloboside antibody. KU812Ep6 cells were infected with B19 and washed as described. Cells were further incubated for 48 hours at 37°C and washed with PBS 3 times before the quantitative study of B19 DNA. To activate α5β1 integrin, anti-integrin antibodies were used in the presence of divalent ions (1 mM Mn^{2+}, 1 mM Mg^{2+}). The blocking ability of B19 replication by each antibody was expressed as described. $^{**}P < .01$, $^{*}P < .05$ by Student *t* test. (D) RNA interference of Ku80 in KU812Ep6 cells. Cell-surface expression of Ku80 was examined by flow cytometry in scramble RNA or siRNA of Ku80-transfected KU812Ep6 cells (left panel). KU812Ep6 cells treated with indicated RNA were reacted with 5 μg/mL mouse monoclonal anti-Ku80 antibody or 5 μg/mL isotype-matched mouse monoclonal antibody 1F5 (shadow), followed by FITC-labeled anti–mouse IgG antibodies. B19 association of siRNA-transfected KU812Ep6 cells was evaluated by quantitative PCR (right panel). Sample DNA was prepared from extensively washed scramble RNA or siRNA of Ku80-transfected KU812Ep6 cells after 2 hours of incubation with B19. $^{*}P < .01$ by Student *t* test.

Ku80 functions as a coreceptor for B19 infection together with P antigen

We then performed an inhibition test for B19 infection of KU812Ep6 cells using antibodies against Ku80, P antigen, α5β1 integrin. Anti-Ku80 antibody inhibited B19 binding, whereas anti-P antibody, GL4, did not inhibit B19 binding. Anti–α5 and anti–β1

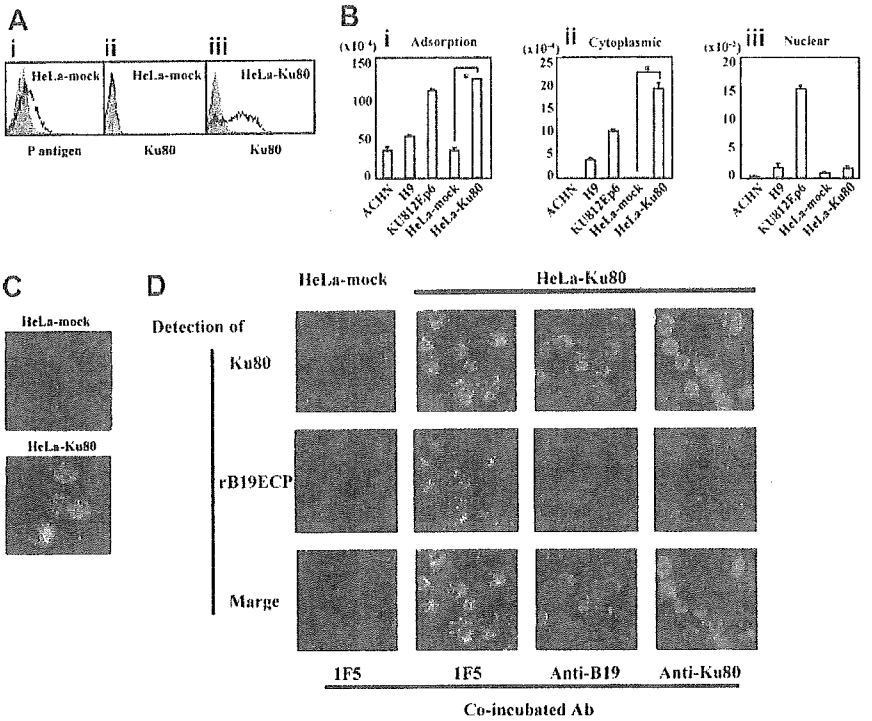

Figure 5. Transfection of Ku80 to HeLa cells. (A) Expression of Ku80 on HeLa cells transfected with pKu80. Ku80 cDNA was inserted to expression plasmid pcD and the resulted pKu80 was transfected to HeLa cells (HeLa-Ku80) using lipofectin. Empty pcD was used for a mock transfection (HeLa-mock). The transfected cells (2×10^5) were incubated with 5 μg/mL of each antibody, anti-Ku80 antibody (ii,iii), GL4 (A1), or isotype-matched mouse monoclonal antibodies or rabbit serum (shadow), and then analyzed for the expression of P antigen or Ku80 on the cell surface. Figures show HeLa-mock expressed P antigen but not Ku antigen on the surface (i,ii), whereas HeLa-Ku80 expressed Ku80 (iii). (B) Increased binding and viral entry of B19 in HeLa-Ku80. The indicated cells (6×10^5) were infected with B19 (2×10^{11} copies of B19 DNA) for 30 minutes on ice. After washing cells 3 times with PBS, pH 7.2, DNA was extracted from 2×10^5 cells. Remaining cells were further incubated for 30 minutes at 37°C. After washing cells 3 times with PBS, pH 4.5, a cytoplasmic and nuclear fraction was prepared, and then DNA was extracted from each fraction. Prepared DNA was subjected to a quantitative PCR to quantify B19 DNA. *$P < .01$ by Student t test. (C) B19 infection to HeLa-Ku80. HeLa-mock or HeLa-Ku80 cells (2×10^5) were infected with B19 (2×10^{11} copies of B19 DNA) for 30 minutes at 37°C. After being washed 3 times with PBS, cells were collected with 5 mM EDTA-PBS, pH 7.2, fixed with 4% paraformaldehyde and reacted with PAR3, followed by FITC-labeled anti–mouse IgG antibody as a secondary antibody. Thus prepared cells were then subjected to a confocal microscope analysis. The panel represents B19 entered into HeLa-Ku80. (D) Colocalization of rB19ECP and Ku80. HeLa-mock or HeLa-Ku80 (2×10^5) cells were incubated with biotinylated rB19ECP (1 μg/mL) in the presence of 5 μg/mL inhibitor antibody indicated for 30 minutes at 37°C. After being washed 3 times with PBS, pH 7.2, cells were collected with 5 mM EDTA-PBS, and rB19ECP or Ku80 was detected by confocal microscopy analysis. Ku80 was detected by anti-Ku80 antibody followed by TRITC-labeled anti–mouse IgG antibody as a secondary antibody. Detection of biotinylated rB19ECP was done by avidin-FITC as described in "Materials and methods."

integrin antibodies caused a slight inhibition of B19 binding (Figure 4B). Both anti-Ku80 antibody and GL4 also inhibited B19 replication in KU812Ep6 cells. The simultaneous presence of both antibodies more strongly inhibited the replication of B19 DNA (Figure 4C). Presence of anti–α5 and anti–β1 integrin antibodies caused only a slight inhibition of B19 replication (Figure 4C). In other experiments, KU812Ep6 cells were treated with siRNA against Ku80 and then tested for the replication of B19 at B19 infection study. The results revealed the suppression of B19 binding to the KU812Ep6 cells with reduced expression of Ku80 (Figure 4D).

The role of Ku80 as a coreceptor for B19 infection was also supported by a transfection experiment using HeLa cells that were nonpermissive for B19 infection. Figure 5A shows that the surface of Ku80-transfected HeLa cells (HeLa-Ku80) became positive for Ku80 expression and binding of B19 to the cells was significantly enhanced (Figure 5B). Quantitative analysis of B19 DNA (Figure 5B) and confocal laser microscopy (Figure 5C) confirmed that B19 DNA and B19 protein were present in the cytoplasmic fraction of HeLa-Ku80 cells 30 minutes after infection, similar to Ku812Ep6. Furthermore, a coincubation experiment of rB19ECP and HeLa-Ku80 revealed the colocalization of rB19ECP and Ku80 in the cytoplasm or membrane (or both) of HeLa-Ku80 (Figure 5D). Moreover, association of rB19ECP and HeLa-Ku80 was apparently inhibited by the presence of anti-B19 antibody or anti-Ku80 antibody (Figure 5D).

Ku80 is expressed on the surface of bone marrow cells

Because Ku80 is known as a nuclear protein, it is important to determine whether or not Ku80 is expressed on the cell-surface in vivo. Ku80 was not detected on the cell surface of peripheral blood mononuclear cells (data not shown). We then examined cell-surface expression of Ku80 in bone marrow cells because bone marrow cells are potential targets of B19 infection. Flow cytometry analysis of bone marrow cells demonstrated that Ku80 was highly expressed on the cell surface of erythroid progenitor cells expressing glycophorin A as well as on the surface of immune cells such as $CD20^+$, $CD3^+$, or $CD14^+$ cells in bone marrow (Figure 6A). A small portion (5.6%) of $CD36^+$ bone marrow cells, which may be permissive to B19 infection,[23] were also positive for the expression of Ku80 on the cell surface (Figure 6B). B19 binding to bone marrow cells was inhibited in the presence of anti-Ku80 antibody at B19 infection in vitro (data not shown). Figure 7 shows that the replication of B19 in bone marrow cells was significantly inhibited in the presence of anti-Ku80 antibody or GL4. The inhibition rate of B19 replication in the presence of both anti-Ku80 antibody and GL4 was similar to that in the presence of GL4.

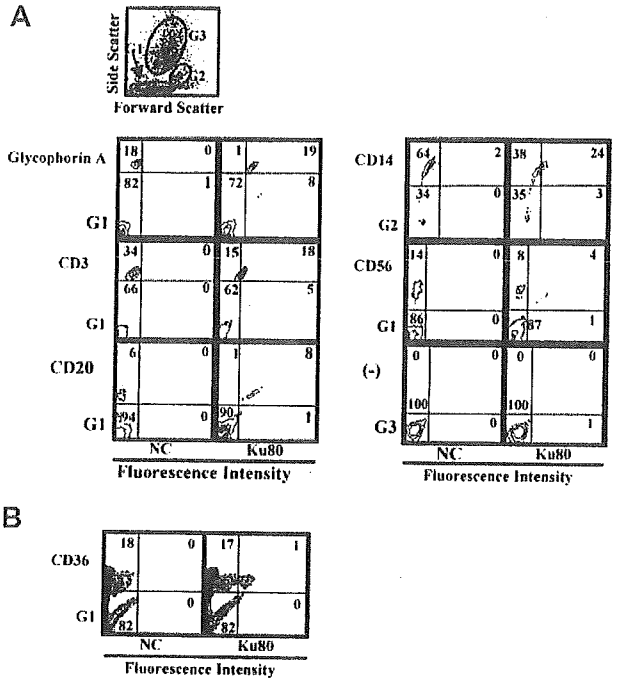

Figure 6. Cell-surface expression of Ku80 in human bone marrow cells. Flow cytometry analysis of Ku80 expression on the cell surface. Bone marrow cells were reacted with indicated antibodies and anti-Ku80 antibody as described in "Materials and methods," and then the expression of surface molecules was analyzed. Prior to the study, each sample had been analyzed by the scattered plot. The results showed that the glycophorin A^+, $CD3^+$, $CD20^+$, $CD56^+$, or $CD36^+$ cells were scattered in gate 1 (G1), and $CD14^+$ cells in gate 2 (G2), and that there were no glycophorin A^+, $CD3^+$, $CD20^+$, $CD56^+$, or $CD36^+$ cells in gate 3 (G3). Then the expression of Ku80 on cell surface in gated cells was analyzed. The gate used in each experiment is shown at left-lower side of each plot. (A) Gates used in the experiment and detection of Ku80 on the surface of various cell lineages. (B) Detection of Ku80 on the surface of $CD36^+$ bone marrow cells.

Discussion

The presented data implicate Ku80 as a coreceptor involved in B19 infection. U937, H9, and ACHN cells expressing Ku80 showed B19 binding, but some cells with P antigen failed to bind B19 unless these cells expressed Ku80 on their surface. A marked increase in B19 binding in Ku80-transfected HeLa cells and the inhibition of B19 infectivity by anti-Ku80 antibody or siRNA to Ku80 suggests a Ku80-dependent B19 interaction with the targeted cells. Specific inhibition of B19 binding by anti-Ku80 antibody that recognized the N-terminus of the Ku80 protein suggests that B19 interacts with specific sites of Ku80 on the cell surface. Further, Epstein-Barr virus or hepatitis virus C failed to bind either to Ku80-expressing HeLa or U937 cells (data not shown). These results suggest that Ku80 is one of the specific receptors for B19 infection.

Ku is a heterodimeric DNA-binding protein consisting of a 70-kDa (Ku70) and an 80-kDa (Ku80) subunit and was originally identified as a nuclear antigen recognized by autoantibodies in patients with systemic lupus erythematosus and scleroderma.[25] Ku has a central role in multiple nuclear processes, including DNA repair, chromosome maintenance, transcription regulation, and V(D)J recombination. Ku is abundant in the nucleus, consistent with its function as a DNA-protein kinase (DNA-PK).[26,27] However, recent studies have shown cytoplasm or surface localization of Ku in various types of cells, including of leukemia, multiple myeloma, and tumor cell lines. Ku is a component of the DNA-PK complex in membrane rafts of mammalian cells.[26] Although the role of surface Ku80 has not been well clarified,[28] signal transduction and Ku80 are coupled in both B and T cells,[25,28,29] and localization of the DNA-PK complex in lipid rafts suggests a putative role in the signal transduction pathway following ionizing radiation.[26] It was recently reported that Ku interacts with metalloproteinase 9 at the cell surface of highly invasive hematopoietic cells of normal and tumor cell origin, and Ku80/MMP-9 interaction at the cell membrane may result in contribution to the invasion of tumor cells through regulation of extracellular matrix remodelling.[30] Further, the membrane form of Ku, whose expression is induced at hypoxia, mediates cell adhesion of plasma cells,[30-32] indicating a role for Ku as an adhesion receptor for fibronectin.[33] The present study showed that Ku80 is positive on the surface of $CD3^+$ cells, $CD20^-$ cells. $CD14^+$ cells, glycophorin A^- cells, and $CD36^+$ cells from bone marrow where B19 infection is permissive.

We have discovered a novel role of Ku80 as a cellular receptor in B19 infection. Anti-Ku80 antibody, however, did not cause complete inhibition of B19 infection, whereas pretreatment with anti-Ku80 antibody together with GL4 strongly inhibited B19 infectivity in KU812Ep6 cells and human bone marrow cells, showing the necessity of P antigen as a receptor. A recent report showed that $\alpha5\beta1$ integrin has a role in B19 entry into host cells,[6] and KU812Ep6, U937, H9, ACHN, and HeLa cells all expressed $\alpha5\beta1$ integrin on their surface (data not shown). However, B19 entry into U937- and H9-expressing Ku80 and $\alpha5\beta1$ integrin or HeLa cells with P antigen and $\alpha5\beta1$ integrin was insufficient or negative (Figures 1 and 5B). B19 entry was marked in KU812Ep6 cells or Ku80-HeLa cells that expressed Ku80, P antigen, and $\alpha5\beta1$ integrin on their surface, showing the necessity of P antigen for efficient binding and the virus entry afterward. Anti-$\alpha5$ and anti-$\beta1$ integrin antibodies, which inhibited the entry of B19 into K562 cells,[6] caused a slight inhibition of B19 binding as well as B19 replication in KU812Ep6, supporting the participation of $\alpha5\beta1$ integrin in B19 infection. We are currently investigating the precise mechanism of the interaction among B19-related receptors such as P antigen, Ku80, and $\alpha5\beta1$ integrin in association with the following signal transduction in B19-infected cells.

The use of multiple receptors for entry into cells has been observed frequently in virus infection, such as by α herpesviruses, HHV-8 or HIV.[34,35] We have shown that B19 uses at least 2 receptors, Ku80 and P antigen, in the process of infection. Ku80

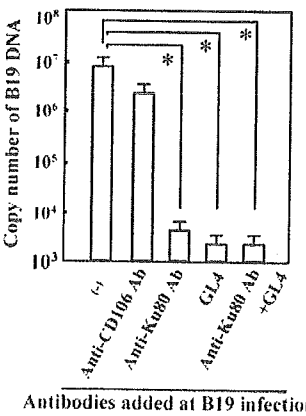

Figure 7. Blocking of B19 infection of bone marrow cells by anti-Ku80 antibody or antiglioboside antibody. Bone marrow cells (2×10^6) were infected with B19 (2×10^{11} copies of B19 DNA) with the indicated antibodies and evaluated for quantity of B19 DNA as described. Anti-CD106 antibody was a mouse monoclonal antibody used as a negative control. The differences in the results between control (−) and other samples were statistically analyzed. $^*P < .01$ by Student *t* test.

may function as an efficient B19-capturing molecule on the cell surface and may also contribute to B19 entry into cells; markedly enhanced entry of B19 in Ku80-HeLa cells (Figure 5C-D) suggests that Ku80 mediates efficient B19 entry in cooperation with P antigen and probably with α5β1 integrin.[6] Although Ku80 can interact with Epstein-Barr virus protein in the nucleus,[36] this study is the first to show the use of Ku80 antigen as a cellular receptor for virus infection. Despite marked entry of B19, synthesis of B19 protein was unsuccessful in Ku80-HeLa cells, but was possible only in erythroid cell lines, indicating that unknown intracellular factors may be required for B19 replication in the targeted cells.[37,38]

Ku80 is not found in circulating mononuclear cells from healthy volunteers but is positive on the surface of B19-binding cells in vivo, such as immune cells in tonsils, erythroblasts, T cells, B cells, macrophages in bone marrow, and immune cells including follicular dendritic cells in rheumatoid joints, indicating the surface expression of Ku antigen may be restricted by environmental conditions. Of interest is that the oxygen levels are markedly low in bone marrow and joints[39-41] compared with that in blood, and surface Ku80 is inducible with hypoxia.[31,32] A recent study suggests the efficiency of B19 infection increases with hypoxia.[42] These studies suggest that surface Ku80 induced with hypoxia may participate in the process of B19 infection of joints and bone marrow.

Ku80 expression on the surface of immune cells in bone marrow in vivo may explain clinical findings associated with B19 infection to nonerythroid cells. Namely, B19 infection often causes a decreased number of leukocytes or lymphocytes in blood during acute B19 infection, as well as increased levels of TNF-α and IFN-γ in blood or rheumatoid joints, and the detection of B19 on T cells, B cells, or macrophages in tonsils, bone marrow, or rheumatoid joints. B19 may infect immune cells in bone marrow or the synovium and persist to lead to secrete an inflammatory cytokine through the activation of AP1 and AP2 by B19 NS1.[43] Stimulation of cellular receptors with B19 may trigger activation of signal cascades in host cells, which may explain why immune cells in acute and prolonged B19 infection or in the joints of rheumatoid arthritis are functionally altered.

Acknowledgments

We are grateful to E. Miyagawa for KU812Ep6, K. Kamata for rB19ECP, T. Mimori for rKu80 and rKu70, C. Morimoto for sCD26, K. Yamaguchi for purified B19, and S. Shibahara for the pKu80.

References

1. Anderson MJ, Jones SE, Fisher-Hoch SP, et al. Human parvovirus, the cause of erythema infectiosum (fifth disease) [letter]? Lancet. 1983;1:1387.
2. Brown KE, Young NS. Parvovirus B19 in human disease. Annu Rev Med. 1997;48:59-67.
3. Brown KE, Anderson SM, Young NS. Erythrocyte P antigen: cellular receptor for B19 parvovirus. Science. 1993;262:114-117.
4. Weigel-Kelly KA, Yoder MC, Srivastava A. Recombinant human parvovirus B19 vectors: erythrocyte P antigen is necessary but not sufficient for successful transduction of human hematopoietic cells. J Virol. 2001;75:4110-4116.
5. Kaufmann B, Baxa U, Chipman PR, Rossmann MG, Modrow S, Seckler R. Parvovirus B19 does not bind to membrane-associated globoside in vitro. Virology. 2005;332:189-198.
6. Weigel-Kelley KA, Yoder MC, Srivastava A. α5β1 integrin as a cellular co-receptor for human parvovirus B19: requirement of functional activation of {beta} 1 integrin for viral entry. Blood. 2003; 102:3927-3933.
7. Wagner AD, Goronzy JJ, Matteson EL, Weyand CM. Systemic monocyte and T cell activation in a patient with human parvovirus B19 infection. Mayo Clin Proc. 1995;70:261-265.
8. Murai C, Munakata Y, Takahashi Y, et al. Rheumatoid arthritis after human parvovirus B19 infection. Ann Rheum Dis. 1999;58:130-132.
9. Anderson MJ, Higgins PG, Davis LR, et al. Experimental parvovirus infection in humans. J Infect Dis. 1985;152:257-265.
10. Barlow GD, Mckendrick MW. Parvovirus B19 causing leucopenia and neutropenia in a healthy adult. J Infect. 2000;40:192-195.
11. Nesher G, Osborn TG, Moore TL. Parvovirus infection mimicking systemic lupus erythematosus. Semin Arthritis Rheum. 1995;24:297-303.
12. Kerr JR, Barah F, Mattey DL, et al. Circulating tumor necrosis factor-α and interferon-γ are detectable during acute and convalent parvovirus B19 infection and are associated with prolonged and chronic fatigue. J Gen Virol. 2001;82:3011-3019.
13. Soderlund M. Persistence of parvovirus B19 DNA in synovial membranes of young patients with and without chronic arthropathy. Lancet. 1997; 349:1063-1065.
14. Takahashi Y, Murai C, Munakata Y, et al. Human parvovirus B19 as a causative agent for rheumatoid arthritis. Proc Natl Acad Sci U S A. 1998;95: 8227-8232.
15. Miyagawa E, Yoshida T, Takahashi H, et al. Infection of the erythroid cell line, KU812Ep6 with human parvovirus B19 and its application to titration of B19 infectivity. J Virol Methods. 1999;83:45-54.
16. Saito T, Munakata Y, Fu Y, et al. Evaluation of anti-parvovirus B19 activity in sera by assay using quantitative polymerase chain reaction. J Virol Methods. 2003;107:81-87.
17. Yamaguchi K, Miyagawa E, Dan M, Miyazaki T, Ikeda H. Cellulose hollowfibers (BMMS) used in the filter membrane can trap human parvovirus B19 [abstract]. Electron Microsc. 2002;2:115.
18. Kajigaya S, Shimada T, Fujita S, Young NS. Self-assembled B19 parvovirus capsids, produced in a baculovirus system, are antigenically and immunogenically similar to native virions. Proc Natl Acad Sci U S A. 1991;88:4646-4650.
19. Yaegashi N, Tada K, Shiraishi H, Ishii T, Nagata K, Sugamura K. Characterization of monoclonal antibodies against human parvovirus B19. Microbiol Immunol. 1989;33:561-567.
20. Brown CS, Jensen T, Meloen RH, et al. Localization of an immunodominant domain on baculovirus produced parvovirus B19 capsids: correlation to a major surface region on the native virus particle. J Virol. 1992;66:6989-6996.
21. Harata N, Sasaki T, Osaki H, et al. Therapeutic treatment of New Zealand mouse disease by a limited number of anti-idiotypic antibodies conjugated with neocarzinostatin. J Clin Invest. 1990; 86:769-776.
22. Okayama H, Berg P. A cDNA cloning vector that permits expression of cDNA inserts in mammalian cells. Mol Cell Biol. 1983;3:280-289.
23. Tanaka T, Duke-Cohen JS, Kameoka J, et al. Enhancement of antigen-induced T-cell proliferation by soluble CD26/dispetidyl peptidase IV. Proc Natl Acad Sci U S A. 1994;91:3082-3086.
24. Morey AL, Fleming KA. Immunophenotyping of fetal haematopoietic cells permissive for human parvovirus B19 replication in vitro. Br J Haematol. 1992;82:302-309.
25. Mimori T, Ohosone Y, Hama N, et al. Isolation and characterization of cDNA encoding the 80-kDa subunit protein of the human autoantigen Ku(p70/p80) recognized by autoantibodies from patients with scleroderma-polymyositis overlap syndrome. Proc Natl Acad Sci U S A. 1990;87: 1777-1781.
26. Adam L, Bandyopadhyay D, Kumar R. Interferon-α signaling promotes nucleus-to-cytoplasmic redistribution of p95Vav, and formation of a multisubunit complex involving Vav, Ku80, and Trk-2. Biochem Biophys Res Commun. 2000;267:692-696.
27. Hector L, Darren G, Guillermo ET. Novel localization of the DNA-PK complex in lipid rafts. J Biol Chem. 2003;278:22136-22143.
28. Prabhakar BS, Allaway GP, Srinivasappa J, Notkins AL. Cell surface expression of the 70-kD component of Ku, a DNA-binding nuclear autoantigen. J Clin Invest. 1990;86:1301-1305.
29. Morio T, Hanissian SH, Bacharier LB, et al. Ku in the cytoplasm associates with CD40 in human B cells and translocates into the nucleus following incubation with IL-4 and anti-CD40 mAb. Immunity. 1999;11:339-348.
30. Monferran S, Paupert J, Dauvillier S, Salles B, Muller C. The membrane form of the DNA repair protein Ku interacts at the cell surface with metalloproteinase 9. EMBO J. 2004;23:3758-3768.
31. Teoh G, Urashima M, Greenfield EA, et al. The 86-kD subunit of Ku autoantigen mediates homotypic and heterotypic adhesion of multiple myeloma cells. J Clin Invest. 1998;101:1379-1388.
32. Lynch EM, Moreland RB, Ginis I, Perrine SP, Faller DV. Hypoxia-activated ligand HAL1/13 is lupus autoantigen Ku80 and mediates lymphoid cell adhesion in vitro. Am J Physiol Cell Physiol. 2001;280:897-911.
33. Sylvie M, Catherine M, Lionel M, Philippe F, Bernard S. The membrane-associated form of the DNA repair protein Ku is involved in cell

adhesion to fibronectin. J Mol Biol. 2004;26: 503-511.

34. Spear PG, Eisenberg RJ, Cohen GH. Three classes of cell surface receptors for alphaherpesvirus entry. Virology. 2000;275:1-8.
35. Shaw MA, Naranatt PP, Fu ZW, Bala C. Integrin α3β1(CD49c/29) is a cellular receptor for Kaposi's sarcoma-associated herpesvirus (KSHV/HHV-8) entry into the T cells. Cell. 2002;108:407-419.
36. Shieh B, Schultz J, Guinness M, Lacy J. Regulation of the human IgE receptor (Fc epsilonRIII/CD23) by Epstein-Barr virus (EBV): Ku autoantigen binds specifically to an EBV-responsive enhancer of CD23. Int Immunol. 1997;9:1885-1895.
37. Liu JM, Green SW, Shimada T, Young NS. A block in full-length transcript maturation in cells nonpermissive for B19 parvovirus. J Virol. 1992;66: 4686-4692.
38. Brunstein J, Soderlund VM, Hedman K. Identification of a novel splicing pattern as a basis of restricted tropism of erythrovirus B19. Virology. 2000;274: 284-291.
39. Bodamyali T, Stevens CR, Billingham MEJ, Ohta S, Blake DR. Influence of hypoxia in inflammatory synovitis. Ann Rheum Dis. 1998;57: 703-710.
40. Harrison SJ, Rameshwer P, Chang V, Bandari P. Oxygen saturation in the bone marrow of healthy volunteers [letter]. Blood. 2002;99:394.
41. Cernanec J, Guilak F, Weinberg JB, Piestsky DS, Fermor B. Influence of hypoxia and reoxygenation on cytokine-induced production of proinflammatory mediators in articular cartilage. Arthritis Rheum. 2002;46:968-975.
42. Piellet S, Guyader NL, Hofer T, et al. Hypoxia enhances human B19 erythrovirus gene expression in primary erythroid cells. Virology. 2004;327:1-7.
43. Fu Y, Ishii KK, Munakata Y, Saito T, Kaku M, Sasaki T. Regulation of tumor necrosis factor α promoter by human parvovirus B19 NS1 through activation of AP1 and AP2. J Virol. 2002;76:5359-5365.

11

Oxidative Stress in Rheumatoid Arthritis

TAKASHI OKAMOTO
Department of Molecular and Cellular Biology,
Nagoya City University, Nagoya, Japan

I. INTRODUCTION

Reactive oxygen species (ROS) are produced in the cells by various environmental stimuli such as infection of microbes (viruses, bacteria, etc.), ionizing and UV irradiation, and pollutants (i.e., oxidants), which are collectively called "oxidative stress." These environmental challenges elicit inflammatory and immune responses (1). Interestingly, these factors are also regarded as risk factors and disease-accelerating factors for autoimmune diseases including rheumatoid arthritis (RA) (Fig. 1). In addition, inflammatory responses in F1
mammals are often associated with ROS production from neutrophils and macrophages. Therefore, this natural

such as TNFα, IL1, IL-6, IL-8, IL-12, IL-16, IL-18, and IFNγ (reviewed in Refs. 2–5).

II. PATHOPHYSIOLOGY OF RA

Proposed causes for RA include: (i) genetic preposition; (ii) pathogenetic immuno-inflammatory responses triggered by environmental agents, particularly microbes; (iii) autoimmunity directed against components of synovium and cartilage; (iv) dysregulated production of cytokines; (v) recruitment of immuno-inflammatory cells through induction of inflammatory cell adhesion molecules (e.g., E-selectin, ICAM-1, and VCAM-1); and (vi) transformation of synovial cells into autonomously proliferating cells with tissue-infiltrating nature [often referred to as "transformed-like" phenotype (7)]. We have recently clarified the transformed-like nature of rheumatoid synoviocytes by performing gene expression profile analyses of synoviocytes and elucidated cellular genes specifically activated in RA synoviocytes (8,9). When compared with control synoviocytes obtained from healthy individuals (upon injury) or osteoarthritis (OA) patients, we found that both PDGF receptor α and SDF-1, a chemokine, genes are activated in RA synoviocytes without any external stimulus (8). Interestingly, from the gene knockout studies, it was shown that these factors are required for the development of limb joints. Moreover, when synoviocytes were stimulated with physiological concentration of TNFα, a principal proinflammatory cytokine, cell fate-determining factors, including Notch 1, Notch 4, and Jagged-2, a ligand for Notch proteins were activated only in RA synoviocytes (9). These findings indicate that RA synoviocytes may have reacquired the "revertant" phenotype mimicking the primordial synoviocytes that exhibit hyperproliferation and invasion, at least in a part. It is possible that this peculiar feature is caused by the long-term inflammatory stimulation, through which constitutive activation of particular signaling and transcription pathways lead to the change in "histone code" proposed by Allis (see Ref. 10 for review) and eventually change the epigenetic behavior of cells.

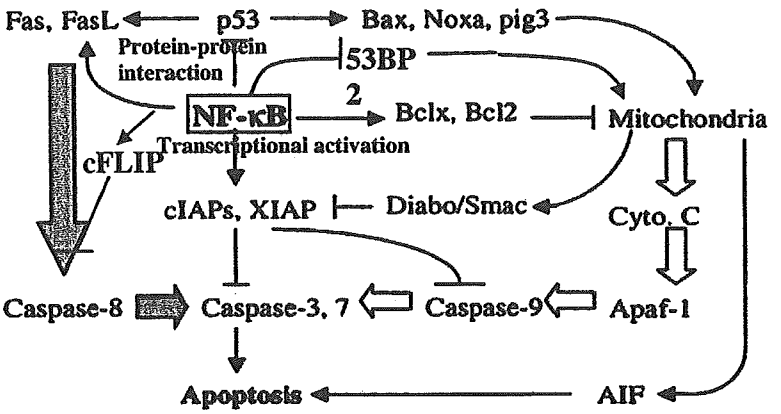

Figure 3 Antiapoptotic actions of NF-κB. Nuclear factor-κB inhibits apoptosis by: (i) transcriptional activation of antiapoptotic factors including cIAPs, XIAP, cFLIP, Bclx, and Bcl2, and (ii) direct inhibition of proapoptotic proteins such as p53 and 53BP2. Oxidation of NF-κB by gold cation. The active DNA binding form of NF-κB is hypothesized to contain zinc ions. When gold compound is added, Au(I) can take the electron from thiolate anions due to its higher oxidation potential compared with that of Zn^{2+}. Thus, Au(I) eventually oxidizes the thiolate anions of NF-κB into disulfide. The oxidation of NF-κB abolishes the DNA-binding activity. AQ1

induces gene expression of cell growth-promoting factors, such as cyclin D1 and c-Myc, and physiological inhibitors of apoptosis, such as cIAPs, Bcl-X_L, and cFLIP (12,13) (Fig. 3). Moreover, it is shown that NF-κB blocks apoptosis in the absence of de novo protein synthesis (14) through protein–protein interaction with p53 and proapoptotic protein 53BP2 (15,16). F3

These actions of NF-κB explain not only the inflammatory responses, but also the hyperproliferation of synovial tissues in RA, indicating that NF-κB acts as a major determinant for RA pathophysiology. Nuclear factor-κB induces TNFα and IL-1β gene expression, and both TNFα and IL-1β stimulate NF-κB signaling; a vicious cycle is formed to perpetuate and even expand the inflammatory responses (11). Thus, the intervention therapy against using anti-TNF antibody and IL-1β receptor antagonist has been developed (17,18). In addition, some of the drugs for RA have been shown to block

As mentioned earlier, the degradation of hyaluronic acid is considered responsible for the decreased viscosity of joint fluid and the increase in intra-articular pressure, and the oxidatively damaged IgG accounts for the generation of reactive epitopes for the production of rheumatoid factor.

V. OXIDO-REDUCTION OF PROTEINS AS A SIGNAL: REDOX REGULATION

Reactive oxygen species are highly reactive with biological macromolecules to result in producing lipid peroxides (which are often radicals), inactivating proteins and mutating DNA (by producing 8-OH-dG or breaking nucleic acid chains). Therefore, cells must have acquired the multiplicated endogenous antioxidant system for the maintenance of a stable form of life under such harmful conditions. These defense mechanisms include reducing enzymes such as thioredoxin (Trx) and glutaredoxin (Grx) (31–33). Oxidized protein molecules by ROS are reversibly reduced by Trx or Grx. Importantly, this reversible oxidation and reduction involving Cys residues of a functional protein sometimes work as a regulatory modification that determines its biological/biochemical activities. This is analogous to the regulatory modification of proteins such as phosphorylation (involving Ser, Thr, and Tyr residues), acetylation and methylation (Lys), and ubiquitination (Lys) (Fig. 4). Thus, the term "redox regulation" has been proposed indicating the active role of oxido-reductive modifications of proteins in regulating their activities. In other words, oxidation and reduction of biomolecules can be regarded as "signals" through which the organism communicates with external environment. There are accumulating evidences indicating that such redox control system works for the maintenance of cellular homeostasis (11,33–35). F4 AQ2

VI. SIGNALING CASCADE FOR NF-κB ACTIVATION

The members of the NF-κB family in mammalian cells include the proto-oncogene c-Rel, RelA (p65), RelB, NFkB1

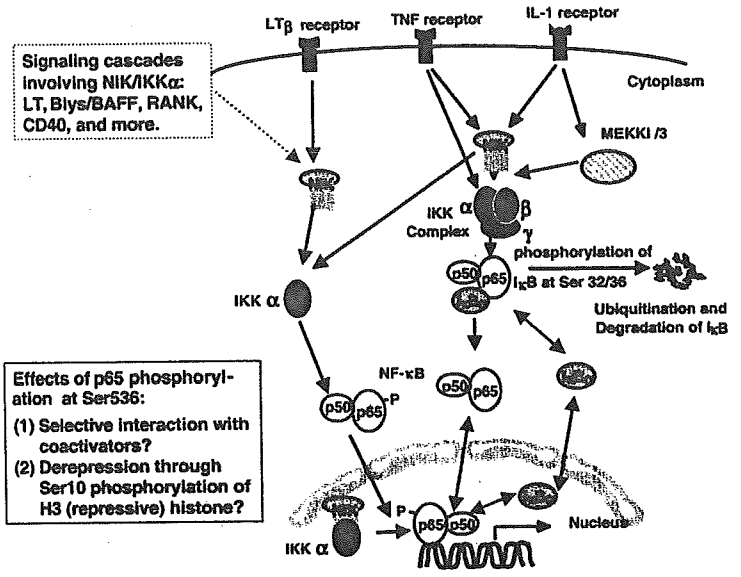

Figure 5 Nuclear factor-κB activation cascades. In addition to canonical pathway involving IκB phosphorylation and ubiquitination followed by its proteolytic degradation in 26S proteasome within the cytoplasm, there appears to be another cascade not involving IκB phosphorylation. Lymphotoxin β receptor signaling, CD40, RANK, and BlyS/BAFF stimulate the NIK–IKKα cascade that leads to p100/p52 processing and p65 phosphorylation at its C-terminal transactivation (Ser536). IKKα also phosphorylates histone H3 in the nucleus and de-represses the otherwise silent nucleosome, thus reactivating the dormant genes. The effect of p65 (Ser536) phosphorylation is considered to activate the transcriptional competence of NF-κB.

phosphorylating serines 32 and 36 of IκBα, was originally identified as ~700 kDa of high molecular complex (29,38,43). Subsequently, two catalytic subunits (IKKα and IKKβ) and a scaffold subunit of this complex (IKKγ/NEMO/IKKAP) were identified and cloned (37,44). The IκB kinase (IKK) complex, consisting of IKKα, β, and γ, can be activated by a variety of stimuli, including TNF-α, IL-1β, and LPS. Activation of the complex involves the phosphorylation of two serine residues located in the "activation loop" within the kinase domain of

corepressor proteins, such as histone deacetylases and Groucho proteins (TLE/AES), and selective interaction with FUS/TLS coactivator protein (58–60). Moreover, recent evidences have demonstrated that upon signaling IKKα translocates to the nucleus and phosphorylates Ser10 of the histone H3 component of nucleosome (61,62) (Fig. 5). Although the histone H3 with methylated Lys9 of H3 renders the local nucleosome to be "repressive," the adjacent Ser10-phosphorylation of H3 histone reverses this effect and de-represses the transcriptional activity of the genes located in the "de-repressed" nucleosome (10).

In addition, it was recently shown that ischemia/reperfusion injury and H_2O_2 induce Src family kinases that subsequently phosphorylate the Tyr42 of IκBα and induce NF-κB in the absence of ubiquitin-dependent degradation (63,64). It appears that Src family kinases act as redox sensors for NF-κB activation. Thus, IKK-independent pathway can function under specific redox-mediated stimuli to activate NF-κB. Although NF-κB activation may reduce tissue damage following the ischemia/reperfusion injury by blocking apoptosis, it may promote synovial cell proliferation in the affected joints of RA patients.

VI.B. Redox Regulation of NF-κB Activation

The induction of NF-κB following liver ischemia/reperfusion injury is regulated by acute redox-activated responses involving an NADPH oxidase Rac1 (65). Other evidences also indicate the involvement of Rac1 in the generation of ROS and activation of NF-κB (66,67). Divergent stimuli that activate NF-κB are considered to generate ROS on the basis of the facts that most such signaling cascades could be blocked by antioxidants, e.g., agents like *N*-acetyl-L-cysteine (NAC), PDTC, and α-lipoic acid were shown to block NF-κB activation in response to diverse stimuli (40,68–72). However, a recent study has clarified that NAC and PDTC block the NF-κB signaling by not necessarily blocking ROS but by lowering the affinity of TNF receptor to its ligand and inhibiting the ubiquitin ligase activity for IκB, respectively (73). No direct evidence of ROS production in response to various NF-κB

AQ3

recognition domain, there is a redox-sensitive Cys (74,75) in the loop of the β-barrel structure that makes a direct contact with the DNA (80,81). Qin et al. (82) has solved the 3D NMR structure of Trx molecule that is associated with the DNA-binding loop of p50 subunit of NF-κB and showed that a redox-active Cys located in the depth of the boot-shaped hollow on Trx surface is in the close proximity with the redox-sensitive Cys of the DNA-binding loop of p50 and likely to reduce the oxidized cysteine on p50 by donating protons in a structure-dependent fashion. However, the inter-molecular disulfide bridge bet-ween Trx and NF-κB must be transient because the binding of Trx to the NF-κB DNA-binding loop prevents the recognition of target DNA. On the basis of biochemical reactions, we have postulated that zinc ion replaces the inter-molecular disulfide bridge and dissociates NF-κB from Trx (11,20,41). In favor of this model, we have demonstrated with cultured rheumatoid synoviocytes that NF-κB and Trx concomitantly migrated to the nucleus during the early phase of the NF-κB activation process induced by TNFα (83). Thioredoxin was relocated in the cytoplasm after 30 min of stimulation, whereas the NF-κB was predominantly present at the nucleus for several hours. Thus, it is possible that NF-κB associates with Trx immediately after dissociation from IκB, translocates to the nucleus together, and dissociates from Trx through displacement of the inter-molecular disulfide by zinc ions.

VII. ROLES OF THIOREDOXIN IN RA PATHOPHYSIOLOGY

In order to examine the roles of Trx in RA, we have measured the Trx level in the joint fluid and explored its effects on the NF-κB activation cascade. Others have elucidated additional roles of Trx in the hyperproliferative nature of rheumatoid synoviocytes.

VII.A. Elevated Trx in the RA Joint Fluid

We found that the serum Trx level was elevated in patients with RA when compared with healthy individuals and AQ4

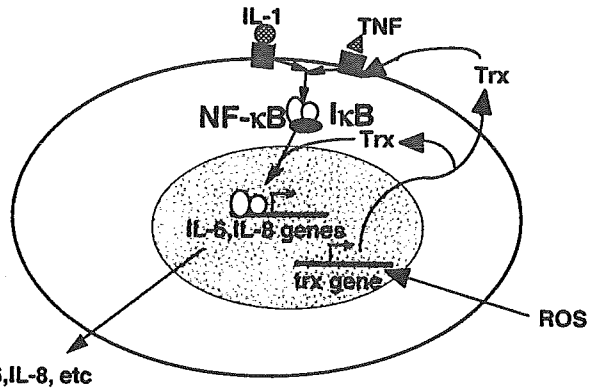

Figure 8 Effect of extracellular Trx on the NF-κB activation stimulated by proinflammatory cytokines. Reactive oxygen species stimulates Trx production in addition to NF-κB activation. See the text for the details.

production in response to TNF-α were greatly augmented by Trx when compared with TNF-α alone (Fig. 8). Furthermore, F8 we found that Trx accelerated the nuclear translocation of NF-κB and facilitated the IκBα phosphorylation and subsequent degradation in response to TNF-α. The elevated Trx level indicates the persistent presence of oxidative stress in the joints of RA patients. Thus, these findings show that Trx has an active role in RA by augmenting the proinflammatory response of TNFα.

VII.B. Regulation of ASK1 Activity by Trx

More intriguingly, another piece of evidence linking the cellular redox status to specific signaling pathways came from the fact that the apoptosis signal regulated kinase 1 (ASK1) interacts with Trx. ASK1 is a member of the MAP3K family that activates downstream kinases including JNK and p38 MAPK. Screening for ASK1-associated proteins using the yeast two-hybrid system led to the identification of Trx as an ASK1-interacting molecule (85). When Trx binds to ASK1, the activity of ASK1 is inhibited (Fig. 9). The rise in ROS F9 levels after TNF-α stimulation leads to activation of ASK1

and act as an antiapoptotic factor, thus supporting the synoviocyte proliferation. However, when excessive ROS is present, due to I/R stress, for example, synoviocytes undergo apoptosis in the presence of severe inflammatory responses. In fact, apoptotic synoviocytes were often observed within the hyperproliferative synovial tissues (refs). AQ5

VIII. CONCLUSION

Rheumatoid arthritis is a complexed process of chronic and progressive inflammation involving numerous transcription factors and signaling molecules. Although majority of pathologic changes of RA appeared to be limited in the joints, similar pathophysiological considerations are applicable to a wide variety of chronic and acute/severe inflammatory diseases including inflammatory bowel diseases, surgical inflammatory response syndrome, multiple sclerosis, and atherosclerosis. In terms of NF-κB involvement, the RA pathophysiology shares with HIV infection and cancer. Thus, findings and therapeutic measures discovered in RA are readily applicable to the understanding and the treatment of these fatal diseases. In other words, when disease processes are broken down into actions of each molecule that governs critical step of many events that build up the entire process, there will be no restriction in applying the concept obtained from the behavior of each molecule to other disease by crossing the border of different scientific disciplines.

ACKNOWLEDGMENT

The author acknowledges the editors of this book for giving me this opportunity to write this review. I owe especially Dr. Lester Packer for his continuous encouragements and everlasting scientific stimulations. This work was supported by grants in aid from the Ministry of Health, Labor and Welfare, the Ministry of Education, Culture, Science and Technology, and from the Japan Health Sciences Foundation.

pathway for NF-κB activation. Curr Top Cell Regul 1997; 35: 149–161.

12. Opferman JT, Korsmeyer SJ. Apoptosis in the development and maintenance of the immune system. Nat Immunol 2003; 4: 410–415.

13. Karin M, Lin A. NF-κB at the crossroads of life and death. Nat Immunol 2002; 3:221–227.

14. Kajino S, Suganuma M, Teranishi F, Takahashi N, Tetsuka T, Ohara H, Itoh M, Okamoto T. Evidence that de novo protein synthesis is dispensable for anti-apoptotic effects of NF-κB. Oncogene 2000; 19:2233–2239.

15. Yang JP, Hori M, Takahashi N, Kawabe T, Kato H, Okamoto T. NF-κB subunit p65 binds to 53BP2 and inhibits cell death induced by 53BP2. Oncogene 1999; 18:5177–5186.

16. Takahashi N, Kobayashi S, Jiang X, Kitagori K, Imai K, Hibi Y, Okamoto T. Expression of 53BP2 and ASPP2 proteins from TP53BP2 gene by alternative splicing. Biochem Biophys Res Commun 2004; 315:434–438.

17. Brennan FM, Chantry D, Jackson A, Maini R, Feldmann M. Inhibitory effect of TNF α antibodies on synovial cell interleukin-1 production in rheumatoid arthritis. Lancet 1989; 2: 244–247.

18. Bresnihan B, Alvaro-Gracia JM, Cobby M, Doherty M, Domljan Z, Emery P, Nuki G, Pavelka K, Rau R, Rozman B, Watt I, Williams B, Aitchison R, McCabe D, Musikic P. Treatment of rheumatoid arthritis with recombinant human interleukin-1 antagonist. Arthritis Rheum 1998; 41:2196–2204.

19. Yamamoto Y, Gaynor RB. Therapeutic potential of inhibition of the NF-κB pathway in the treatment of inflammation and cancer. J Clin Invest 2001; 107:135–142.

20. Yang JP, Merin JP, Nakano T, Kato T, Kitade Y, Okamoto T. Inhibition of the DNA-binding activity of NF-κB by gold compounds in vitro. FEBS Lett 1995; 361:89–96.

21. McKay LI, Cidlowski JA. Molecular control of immune/inflammatory responses: interactions between nuclear factor-κB and steroid receptor-signaling pathways. Endocr Rev 1999; 20: 435–459.

35. Finkel T. Redox-dependent signal transduction. FEBS Lett 2000; 476:52–54.

36. Baldwin AS Jr. Series introduction: the transcription factor NF-κB and human disease. J Clin Invest 2001; 107:3–6.

37. Ghosh S, May MJ, Kopp EB. NF-κB and Rel proteins: evolutionarily conserved mediators of immune responses. Annu Rev Immunol 1998; 16:225–260.

38. Schmitz ML, Bacher S, Kracht M. IκB-independent control of NF-κB activity by modulatory phosphorylations. Trends Biochem Sci 2001; 26:186–190.

39. Karin M, Ben-Neriah Y. Phosphorylation meets ubiquitination: the control of NF-κB activity. Annu Rev Immunol 2000; 18:621–663.

40. Meyer M, Schreck R, Baeuerle PA. H_2O_2 and antioxidants have opposite effects on activation of NF-κB and AP-1 in intact cells: AP-1 as secondary antioxidant-responsive factor. EMBO J 1993; 12:2005–2015.

41. Okamoto T, Tetsuka T. Role of thioredoxin in the redox regulation of gene expression in inflammatory diseases. In: Winyard PG, Blake DR, Evans CH, eds. Free Radicals and Inflammation. Basel: Birkhuser Verlag, 2000:119–131.

42. Saliou C, Kitazawa M, Mclaughlin L, Yang JP, Lodge JK, Iwasaki K, Cillard J, Okamoto T, Packer L. Antioxidants modulate acute solar ultraviolet radiation-induced NF-κB activation in a human keratinocyte cell line. Free Radic Biol Med 1999; 26:174–183.

43. Chen ZJ, Parent L, Maniatis T. Site-specific phosphorylation of IκBα by a novel ubiquitination-dependent protein kinase activity. Cell 1996; 84:853–862.

44. Lee FS, Peters RT, Dang LC, Maniatis T. MEKK1 activates both IκB kinase α and IκB kinase β. Proc Natl Acad Sci USA 1998; 95:9319–9324.

45. Hayashi T, Sekine T, Okamoto T. Identification of a new serine kinase that activates NFκB by direct phosphorylation. J Biol Chem 1993; 268:26790–26795.

in human monocytic cells and endothelial cells. J Biol Chem 1996; 271:20828–20835.

57. Takahashi N, Tetsuka T, Uranishi H, Okamoto T. Inhibition of NF-κB transcriptional activity by protein kinase A. Eur J Biochem 2002; 269:1–7.

58. Uranishi H, Tetsuka T, Yamashita M, Asamitsu K, Shimizu M, Itoh M, Okamoto T. Involvement of the pro-oncoprotein TLS (translocated in liposarcoma) in nuclear factor-κB p65-mediated transcription as a coactivator. J Biol Chem 2001; 276: 13395–13401.

59. Tetsuka T, Uranishi H, Imai H, Ono T, Sonta S, Takahashi N, Asamitsu K, Okamoto T. Inhibition of nuclear factor-κB-mediated transcription by association with the amino-terminal enhancer of split, a Groucho-related protein lacking WD40 repeats. J Biol Chem 2000; 275:4383–4390.

60. Ashburner BP, Westerheide SD, Baldwin AS Jr. The p65 (RelA) subunit of NF-κB interacts with the histone deacetylase (HDAC) corepressors HDAC1 and HDAC2 to negatively regulate gene expression. Mol Cell Biol 2001; 21:7065–7077.

61. Anest V, Hanson JL, Cogswell PC, Steinbrecher KA, Strahl BD, Baldwin AS. A nucleosomal function for IκB kinase-α in NF-κB-dependent gene expression. Nature 2003; 423:659–663.

62. Yamamoto Y, Verma UN, Prajapati S, Kwak YT, Gaynor RB. Histone H3 phosphorylation by IKK-a is critical for cytokine-induced gene expression. Nature 2003; 423:655–659.

63. Imbert V, et al. Tyrosine phosphorylation of IκBα activates NF-κB without proteolytic degradation of IκBα. Cell 1996; 86:787–798.

64. Livolsi A, Busuttil V, Imbert V, Abraham RT, Peyron JF. Tyrosine phosphorylation-dependent activation of NF-κB. Requirement for p56 LCK and ZAP-70 protein tyrosine kinase. Eur J Biochem 2001; 268:1508–1515.

65. Ozaki M, et al. Inhibition of the Rac1 GTPase protects against nonlethal ischemia/reperfusion-induced necrosis and apoptosis in vivo. FASEB J 2000; 14:418–429..

66. Sulciner DJ, Irani K, Yu ZX, Ferrans VJ, Goldschmidt-Clermont P, Finkel T. Rac1 regulates a cytokine-stimulated,